Identification of Distinct Subpopulations of Intercalated Cells in the Mouse Collecting Duct[1]

Patana Teng-umnuay, Jill W. Verlander, Weiping Yuan, C. Craig Tisher, and Kirsten M. Madsen[2]

P. Teng-umnuay, J.W. Verlander, C.C. Tisher, K.M. Madsen, Laboratory of Experimental Morphology, Division of Nephrology, Hypertension and Transplantation, College of Medicine, University of Florida, Gainesville, FL

W. Yuan, Department of Anatomy and Cell Biology, College of Medicine, University of Florida, Gainesville, FL

(J. Am. Soc. Nephrol. 1996; 7:260–274)

ABSTRACT

Structurally and functionally distinct populations of intercalated cells have been described in the collecting duct of both rat and rabbit. However, little is known about these cells in the mouse kidney. The study presented here examines ultrastructural and immunological characteristics of different types of intercalated cells in the mouse. Kidneys of two strains of normal female mice, C57BL/6 and IBR, were preserved by *in vivo* perfusion with 1% glutaraldehyde or paraformaldehyde-picric acid fixatives and processed for morphological evaluation or light and electron microscopic immunohistochemistry, respectively. The avidin-biotin-horseradish peroxidase procedure was performed on wax sections using antibodies against carbonic anhydrase II, H^+-ATPase and Band 3 protein. Immunogold cytochemistry was performed on Lowicryl sections using antibodies to H^+-ATPase and Band 3 protein. Colocalization of H^+-ATPase and Band 3 protein was performed by double labeling using an immunogold technique with silver enhancement. Intercalated cells identified by positive staining for H^+-ATPase and carbonic anhydrase II constituted 35% to 40% of all cells in the connecting tubule (CNT), cortical collecting duct (CCD), and outer medullary collecting duct (OMCD). Type A intercalated cells identified by positive Band 3 staining constituted 16%, 24%, and 33% of the total cell population in the CNT, CCD, and OMCD, respectively. Electron microscopy and immunogold cytochemistry demonstrated three distinct populations of intercalated cells. Type A intercalated cells with apical H^+-ATPase and basolateral Band 3 immunoreactivity were present in all segments examined, and had prominent apical microprojections and characteristic tubulovesicular structures beneath the apical surface, both coated with studs on the cytoplasmic face. Type B intercalated cells with basolateral and cytoplasmic H^+-ATPase and no Band 3 immunoreactivity were most frequently observed in the initial collecting tubule, but were present also in the CNT and early CCD. Type B intercalated cells had a fairly smooth apical surface, a gray zone free of organelles beneath the apical plasma membrane, and small cytoplasmic vesicles without studs throughout the cell. A third type of intercalated cell with apical and cytoplasmic H^+-ATPase, but no basolateral Band 3 protein, was observed exclusively in the CNT and the initial collecting tubule. This type of cell was large, with numerous mitochondria, and vesicles coated with studs were present throughout the cell. It resembled a third type of intercalated cell described previously in the rat. It is concluded that three morphologically and immunologically distinct types of intercalated cells are present in the mouse kidney.

Key Words: *Light microscopy, transmission electron microscopy, carbonic anhydrase, H^+-ATPase, Band 3 protein*

The mammalian collecting duct is an important site of acid secretion and bicarbonate reabsorption. Studies from several laboratories have provided evidence that intercalated cells are responsible for acid-base transport in the collecting duct (1–3). In addition to the collecting duct, intercalated cells are also present in the connecting segment or the connecting tubule (CNT), which is a transitional segment between the distal convoluted tubule and the collecting duct. In the rabbit, the CNT is well demarcated and contains only two main cell types, the CNT cell and the intercalated cell (4). In the rat, the transition is more gradual and the CNT also contains distal convoluted tubule cells and principal cells, in addition to CNT cells and intercalated cells (5,6). The morphology of intercalated cells has been described in detail in both the rabbit (4,7) and the rat (1,2,8). These cells exhibit very distinctive features and have been called "dark cells" because of the presence of a dense-staining cytoplasm that contains numerous mitochondria, polysomes, and tubulovesicular membrane structures.

At least two morphologically and immunologically distinct populations of intercalated cells, Type A and Type B, have been characterized in both the cortical collecting duct (CCD) and the CNT (1,2,6,9). In the rat,

[1] Received August 17, 1995. Accepted November 14, 1995.

[2] Correspondence to Dr. K.M. Madsen, Division of Nephrology, Hypertension, and Transplantation, University of Florida, P.O. Box 100224, Gainesville, FL 32610-0224.

1046-6673/0702-0260$03.00/0
Journal of the American Society of Nephrology

each type of intercalated cell has a distinctive ultrastructural appearance and can be easily identified (1,3). The Type A cell is characterized by the presence of tubulovesicular structures beneath the apical plasma membrane and prominent luminal microprojections. In contrast, the Type B intercalated cell has short luminal microprojections, and small vesicles are distributed throughout a darker-staining cytoplasm (1,3,10). In the rabbit, different configurations of intercalated cells have also been described on the basis of the density of the cytoplasm and the appearance of apical cytoplasmic vesicles (4). However, the ultrastructure of the intercalated cells in the rabbit CCD and CNT can vary widely and it is not possible to clearly separate the cells into two populations on the basis of morphologic criteria alone.

The different populations of intercalated cells have been characterized by both immunohistochemistry and immunocytochemistry by using antibodies against the vacuolar H^+-ATPase, carbonic anhydrase II (CA II), and erythrocyte Band 3 protein. All intercalated cells in both the rat and rabbit exhibit immunostaining for H^+-ATPase. They also contain high levels of CA II (11). In Type A cells in both species, the H^+-ATPase is located in the apical plasma membrane and in apical tubulovesicles, whereas in Type B cells the H^+-ATPase is found in the basolateral plasma membrane and in vesicles scattered diffusely in the cytoplasm (3,12–17). However, in the rabbit, the H^+-ATPase immunolabeling is not as polarized as in the rat, and many intercalated cells do not exhibit plasma membrane labeling (16,17). Band 3 immunoreactivity is present only in Type A intercalated cells and, therefore, can be used as a specific marker for this type of intercalated cell (12,18,19). In the rat, Band 3 immunostaining is located in the basolateral plasma membrane of all Type A cells (19). However, in the rabbit, most Band 3-positive cells in the CCD and CNT also exhibit strong immunostaining in small vesicles and multivesicular bodies (20,21). Type B cells do not possess Band 3 immunoreactivity, thus providing evidence that the apical Cl^-/HCO_3^--exchanger is distinct from the Band 3-like anion exchanger in the Type A cells (17–19).

A third configuration of intercalated cell has also been described in the rat (22). This NonA-NonB type of intercalated cell exhibits positive apical plasma-membrane labeling for H^+-ATPase but does not exhibit basolateral Band 3 immunoreactivity (12).

Early electron microscopic studies by Rhodin (23,24) and Clark (25) described the ultrastructural appearance of intercalated cells in the mouse kidney. However, those studies did not describe different configurations of these cells. Moreover, the functional properties and immunocytochemical characteristics of the intercalated cells in the mouse are not known. Because of the incomplete knowledge of the anatomy of intercalated cells in the mouse collecting duct, and because of increased use of the mouse as a transgenic animal model for the study of kidney disease, this study was designed to identify both ultrastructural and functional characteristics of the different types of intercalated cells in the mouse.

METHODS

Preservation of Tissue for Transmission Electron Microscopy

Five normal adult black female mice, Strain C57BL/6, and five normal adult white female mice, Strain ICR, body weight 17 to 23 grams, were anesthesized with sodium pentobarbital, 50 mg/kg body weight ip. The kidneys were rinsed briefly by perfusion through the abdominal aorta or through the left ventricle with a phosphate-buffered balanced salt solution (PBS) or a Tyrode buffer to remove all blood before being preserved by perfusion with 1% glutaraldehyde in the same buffer solution for 4 min. The kidneys were removed, cut transversely into halves, and immersed in the fixative overnight. Slices of kidney tissue from each animal were divided into specific areas (cortex and outer medulla), and the tissue from each area was cut into 1 to 2 mm^3 blocks. All tissue was postfixed for 1 h in 2% osmium tetroxide in 0.1 M sodium cacodylate buffer, dehydrated through a graded series of ethanol and propylene oxide and embedded in Medcast (Ted Pella, Inc., Redding, CA), an epoxy resin. One-micron sections were cut, stained with toluidine blue, and examined by light microscopy. Thin sections were stained with uranyl acetate in 30% ethanol and lead citrate, and examined with a Zeiss 10A transmission electron microscope (Zeiss, Oberkochen, Germany). At least one grid from the cortex and one grid from the medulla of each animal were studied and all observed intercalated cells were photographed.

Preservation of Tissue for Immunocytochemistry

Six normal adult female white mice, Strain ICR, and six normal adult female black mice, Strain C57BL/6 were studied. The kidneys were perfused through the abdominal aorta or through the left ventricle with PBS and preserved for immunocytochemical studies by perfusion with 2% or 3% paraformaldehyde in PBS containing picric acid for 4 min. The number of animals perfused with 2% or 3% paraformaldehyde was equal (three for each strain). The kidneys were removed, cut transversely into halves, and immersed in the fixative overnight. For light microscopic immunohistochemistry, the kidney slices were dehydrated in graded ethanols and embedded in wax (polyethylene glycol 400 disterate, Polysciences Inc., Warrington, PA). For immunogold cytochemistry, tissue from the cortex was minced into 1-mm^3 samples, rinsed with PBS, dehydrated in graded ethanols, and embedded in Lowicryl K4M (Chemische Werke Lowi, Waldkraiburg, Germany).

Antibodies

CA II was localized by the immunoperoxidase technique using a rabbit polyclonal antibody against mouse erythrocyte CA II at a dilution of 1:1600 for light microscopic immunocytochemistry. The antibody was provided by Dr. Paul Linser, Department of Anatomy and Cell Biology, University of Florida, Gainesville, FL, and has been characterized previously (11,26). Vacuolar H^+-ATPase was localized by using a rabbit polyclonal antibody against the 70 kd catalytic subunit of the H^+-ATPase from bovine brain clathrin-coated vesicles at a dilution of 1:2000 for light microscopic immunohistochemistry and 1:1000 for immunogold cytochemistry. The antibody was provided by Dr. Dennis Stone, Univer-

sity of Texas Health Science Center, Dallas, Texas, and is known to label intercalated cells in the rat and rabbit (16,27,28). The Band 3-like Cl^--HCO_3^--exchanger was localized using a rabbit polyclonal antibody against human erythrocyte Band 3 protein at a dilution of 1:400 for both light microscopic immunohistochemistry and immunogold cytochemistry. The antibody was provided by Dr. Philip Low, Purdue University, West Lafayette, Indiana, and is known to label Type A intercalated cells in the rat (19).

Light Microscopic Immunohistochemistry

The avidin-biotin-horseradish peroxidase complex technique was used. Four μm thick sections were dewaxed, rehydrated, and incubated for 30 min with 3% H_2O_2 to eliminate endogenous peroxidase activity. After being rinsed in PBS, the sections were treated with blocking serum before being incubated with the primary antibody against CA II, H^+-ATPase, or Band 3 protein diluted with 1% BSA in PBS for 60 min. The sections were then rinsed with PBS and incubated with biotinylated goat antirabbit IgG for 30 min. After being rinsed, the sections were incubated with the ABC reagent (Vectastain ABC kit, Vector Laboratories, Burlingame, CA) for 30 min and were then exposed to the peroxidase substrate solution (diaminobenzidine) for 5 min. The sections were washed, counterstained with hematoxylin, and then examined and photographed on a light microscope (Zeiss Photomicroscope II; Zeiss, Oberkochen, Germany). Sections processed in the same way but incubated without primary antibody served as negative controls.

Quantitation of Intercalated Cells

To quantify the different subtypes of intercalated cells in the CNT, CCD, and outer medullary collecting duct (OMCD), the number of cells that exhibited immunoreactivity for CA II, H^+-ATPase, and Band 3 protein were counted on wax sections and expressed as a percentage of the total number of cells in the different tubule segments. For each antibody, cells were counted from one section cut through the entire kidney from each of the 12 animals studied. Areas to be counted were selected in a systematic randomized fashion by using an eyepiece grid, and between 100 and 300 cells were counted from each tubule segment per animal for each antibody. Because principal cells in the OMCD also exhibited weak staining for CA II, we did not count the number of CA II-labeled cells in this segment of the collecting duct.

Immunogold Cytochemistry

The details of this procedure have been described previously (28). Thin sections of Lowicryl-embedded tissues from six animals of each strain were mounted on formvar-coated nickel grids. The grids were treated with 0.1 M NH_4Cl before being incubated overnight at 4°C in a moist chamber with polyclonal rabbit antibodies against H^+-ATPase or human Band 3 protein, diluted in a 10 mM Tris-HCl buffer containing 500 mM NaCl, 0.025% NaN_3, and 1% BSA (pH 7.2). This was followed by incubation with 15 nm gold-conjugated goat antirabbit antibody (GAR) (Auroprobe EM G-15; Amersham Arlington Heights, IL) of 1:50 dilution for 2 h. The grids were counterstained with uranyl acetate and lead citrate and were examined on a Zeiss 10A transmission electron microscope (Zeiss, Oberkochen, Germany).

Colocalization of H^+-ATPase and Band 3 Protein

A silver enhancement technique was used to colocalize H^+-ATPase and Band 3 protein in the intercalated cells. Immunogold cytochemistry with antibodies to H^+-ATPase was performed as described above except 10 nm gold-conjugated GAR (AuroProbe EM G-10; Amersham, Arlington Heights, IL) was used as the secondary antibody. Silver enhancement of the colloidal gold marker of the first antibody was then performed by using established procedures (29,30). In brief, the grids were incubated for 5 min at room temperature in a silver-enhancement reagent (Boehringer Mannheim, Indianapolis, IN), which was prepared immediately before use by mixing developer and enhancer at a ratio of 1:1. After the grids were rinsed with excess distilled water, the second immunogold procedure was performed using anti-Band 3 antibody as the primary antibody as described above and 10 nm gold-conjugated GAR as the secondary antibody. The grids were then counterstained and examined on a Zeiss 10A transmission electron microscope. The labeling of each antibody in the same specimens could be recognized by the difference in size of the gold particles with the larger identifying H^+-ATPase.

RESULTS

Light Microscopy

Three specific tubule segments, including the CNT, the CCD, and the OMCD, were examined on 1-μm plastic sections by light microscopy. Intercalated cells were easily identified by their dark-stained cytoplasm and bulging apical surface, and were present in the CNT as well as in the CCD and OMCD. No differences were observed in the segmental distribution or the morphological appearance of intercalated cells between the two strains of mice. Although the intercalated cells varied in both size and shape, particularly in the CNT and initial CCD, it was not possible to identify subtypes of intercalated cells by light microscopy alone.

Light Microscopic Immunohistochemistry. Light microscopic examination of the sections processed for immunohistochemistry with antibodies against CA II and H^+-ATPase revealed strong and diffuse staining in a subpopulation of cells in the CNT, CCD, OMCD, and the initial inner medullary collecting duct ($IMCD_i$). The intensity of staining for both CA II (Figure 1a) and H^+-ATPase (Figure 1b) was greater in the apical area, and cells with distinct basolateral labeling for H^+-ATPase could not be identified. Positive staining for

Figure 1. Light micrographs illustrating the immunohistochemical identification of intercalated cells in the mouse kidney by using antibodies to carbonic anhydrase II (CA II) (a), H^+-ATPase (b), and Band 3 protein (c and d). Strong diffuse staining for CA II and H^+-ATPase is present in a subpopulation of cells in both the CNT and CCD. A few cells show apical intensification of H^+-ATPase (b). Basolateral staining for Band 3 protein is weak in the CNT and CCD (c) and very strong in the OMCD (d). Note large Band 3-negative cells in the CNT (arrowhead). Magnification, × 480.

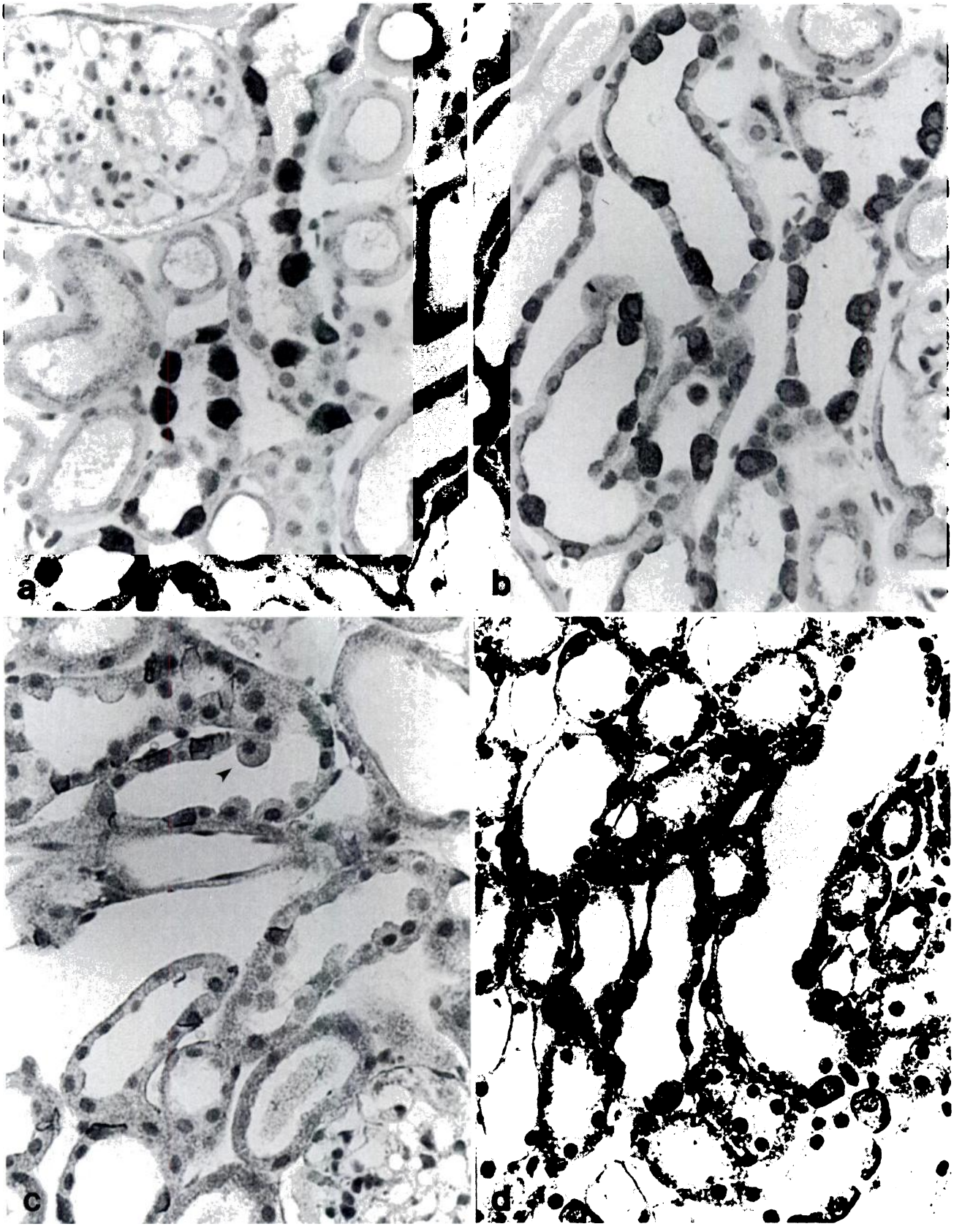
a
b
c
d

TABLE 1. Percentage of collecting duct cells (mean ± SD) labeled for CA II, H^+-ATPase, and Band 3 protein[a]

	CNT	CCD	OMCD
CA II			
ICR strain (N = 6)	36.7 ± 3.06	38.9 ± 3.53	ND
C57BL/6 (N = 6)	37.6 ± 2.20	40.5 ± 2.37	ND
H^+-ATPase			
ICR strain (N = 6)	37.4 ± 1.96	39.4 ± 4.71	35.3 ± 0.89
C57BL/6 (N = 6)	40.7 ± 2.23	39.3 ± 3.15	33.1 ± 2.31
Band 3			
ICR strain (N = 6)	16.6 ± 3.10	25.7 ± 4.86	36.3 ± 3.03
C57BL/6 (N = 6)	15.3 ± 1.83	22.7 ± 2.38	30.6 ± 1.47

[a] CNT, connecting tubule; CCD, cortical collecting duct; OMCD, outer medullary collecting duct; CA II, carbonic anhydrase II.

H^+-ATPase and CA II was also evident in proximal tubules. By using antibody against Band 3 protein, light microscopic examination revealed cells with basolateral staining in the CNT, CCD, OMCD, and $IMCD_i$ (Figures 1c and 1d). The intensity of staining with antibody against Band 3 protein was much stronger in the OMCD and $IMCD_i$ compared with the CNT and CCD. Many large Band 3-negative cells were present in the CNT (Figure 1c). From each animal (six from each strain), cells with positive staining for the different antibodies were counted in the CNT, CCD, and OMCD and expressed as the percentage of the total number of cells counted in the different segments. The results are shown in Table 1. Intercalated cells identified by H^+-ATPase and CA II staining constituted 35% to 40% of the cells in the CNT, CCD, and OMCD in both strains of mice. However, the percentages of Band 3-positive cells, presumed to be Type A intercalated cells, were different for the CNT (15% to 17%), the CCD (23% to 26%), and the OMCD (30% to 36%). Because all of the cells in the OMCD showed positive CA II staining, it was not possible to identify intercalated cells in the OMCD by using this antibody.

Electron Microscopy

Transmission electron microscopy and immunogold cytochemistry with antibodies to the vacuolar H^+-ATPase and erythrocyte Band 3 protein revealed three distinct types of intercalated cells: (*1*) cells with apical plasma membrane and apical vesicle H^+-ATPase and basolateral plasma membrane Band 3 immunoreactivity (Type A cell); (*2*) cells with basolateral plasma membrane and diffuse cytoplasmic vesicle H^+-ATPase and no Band 3 immunoreactivity (Type B cell); and (*3*) cells with apical plasma membrane and cytoplasmic vesicle H^+-ATPase and no Band 3 immunoreactivity (NonA-NonB cell).

Type A Intercalated Cells. The first type of intercalated cell was the most prominent type of intercalated cell in the entire collecting duct, and was distributed from the late distal convoluted tubule and CNT through the CCD, OMCD, and $IMCD_i$. These cells resembled, both morphologically and immunologically, the Type A intercalated cells in the rat. Morphologically, they were characterized by numerous microprojections on the bulging apical surface, and prominent mitochondria distributed generally above, lateral to, and below the nucleus (Figure 2a). Characteristic tubulovesicular structures were located underneath the apical surface, and the cytoplasmic surface of the tubulovesicles and the apical plasma membrane of these cells were coated with studs (Figure 2b). However, the cell shape and the number of microprojections and tubulovesicular structures in the Type A intercalated cells varied from one region to another. In the late distal convoluted tubule and the CNT, the cells were square or rectangular, the apical microprojections were relatively short, and the tubulovesicular structures were less prominent. In the CCD, the cells exhibited a bulging apical surface with prominent microprojections, and numerous tubulovesicular structures were present in the apical cytoplasm. The Type A intercalated cells in the OMCD were intermediate in ultrastructure between those observed in the CNT and the CCD, and had fewer tubulovesicular structures than those in the CCD.

Immunologically, all cells in this group had strong labeling for H^+-ATPase in both the apical plasma membrane and the apical tubulovesicles (Figure 3a). There was no labeling for H^+-ATPase in the basolateral plasma membrane. Distinct labeling for Band 3 protein was present in the basolateral plasma membrane of the cells in this group (Figure 3b), but there was considerable variability in the intensity of labeling between the different segments of the collecting duct. The intensity of labeling gradually increased from the terminal part of the distal convoluted tubule to the OMCD, and was strongest in the OMCD in the inner stripe of the outer medulla. However, in the CCD, some cells with a round shape and long apical microprojections exhibited very strong labeling for Band 3 protein.

Type B Intercalated Cells. The second type of intercalated cell was observed primarily in the initial collecting tubule, but was also present in the late CNT

Figure 2. Transmission electron micrographs of Type A intercalated cell from mouse CCD. The cell is characterized by numerous tubulovesicles in the apical cytoplasm and microprojections on the apical plasma membrane. A high magnification of the cell (b) reveals that the tubulovesicles and regions of the apical plasma membrane are coated with studs. Magnification: (a) × 9200; (b) × 36,100.

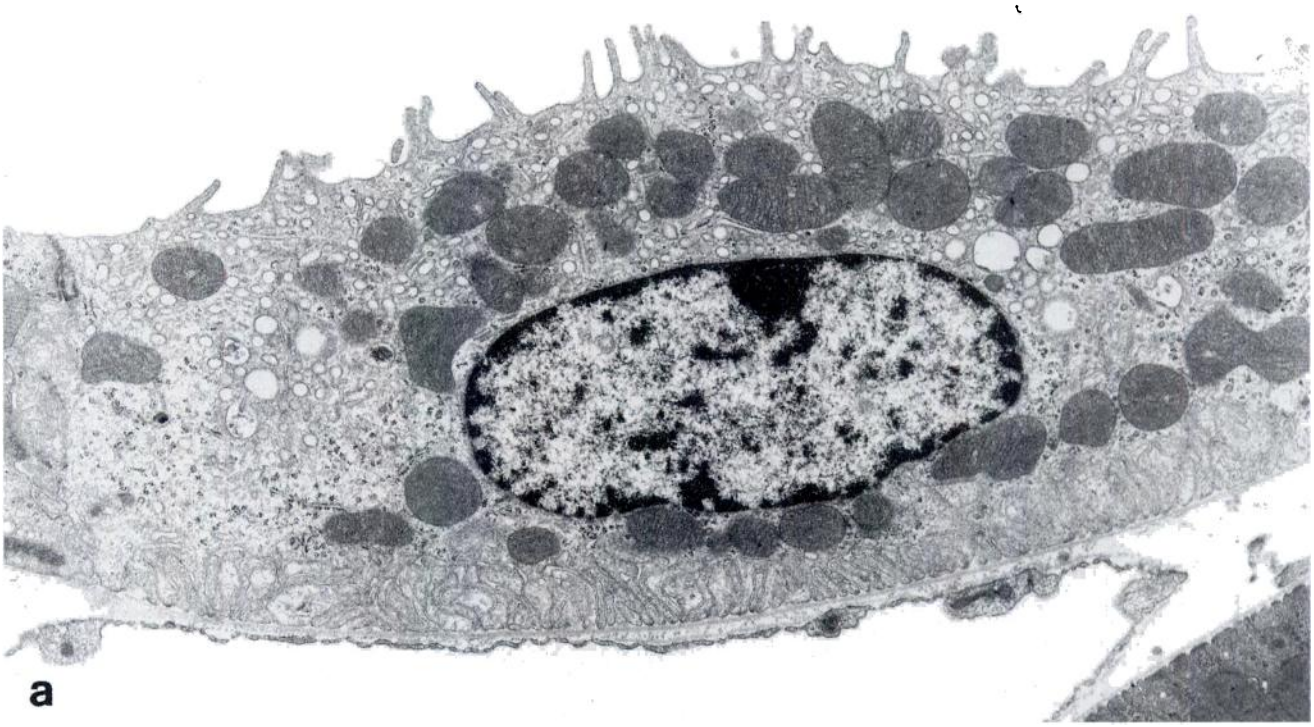
a


b

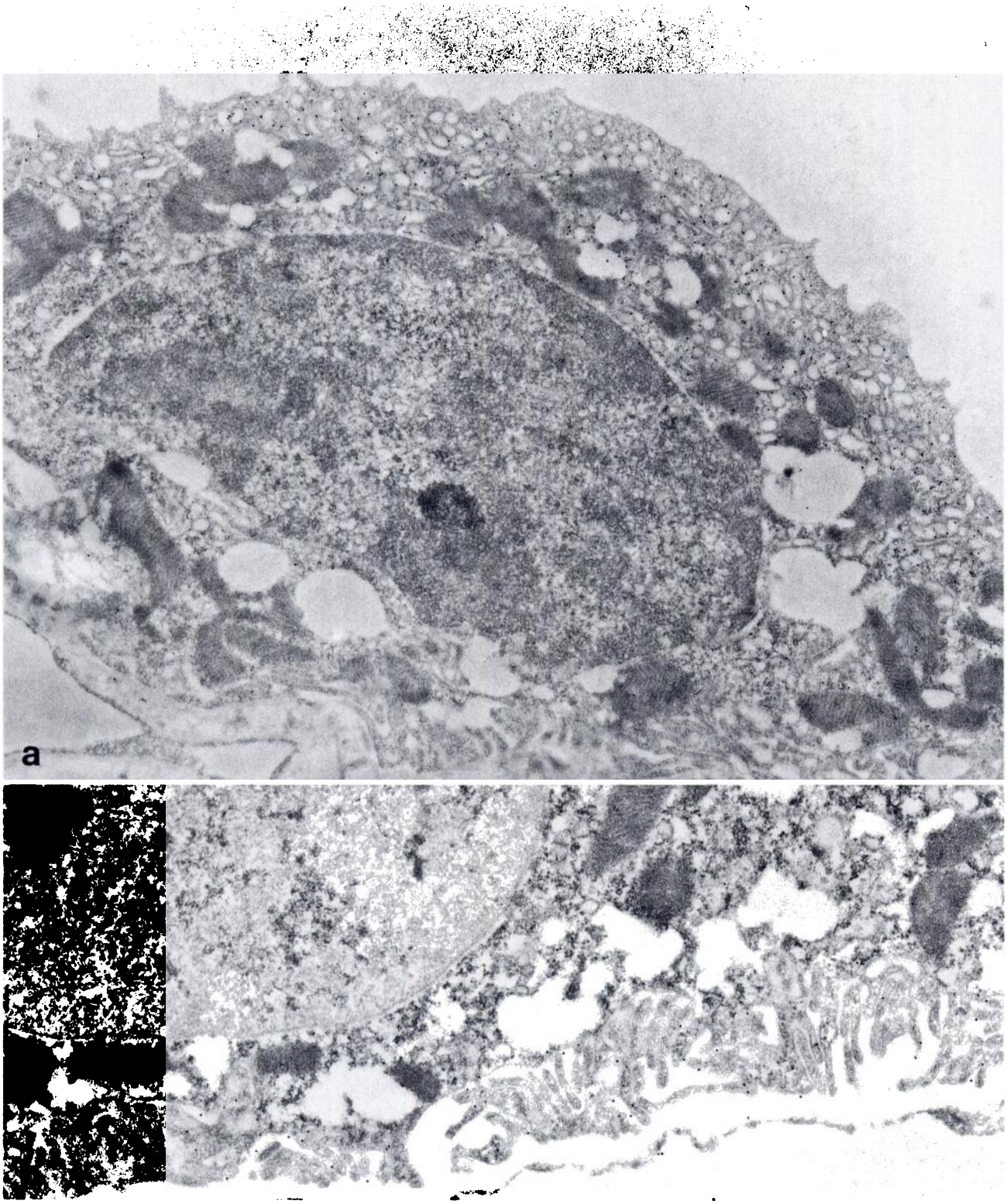

Figure 3. Transmission electron micrographs illustrating immunogold labeling for H^+-ATPase (a) and Band 3 protein (b) in Type A intercalated cells in the mouse CCD. Label for H^+-ATPase is present in the apical plasma membrane and apical tubulovesicles (a) and label for Band 3 protein is present in the basolateral plasma membrane (b). Magnification: (a) × 17,900; (b) × 20,500.

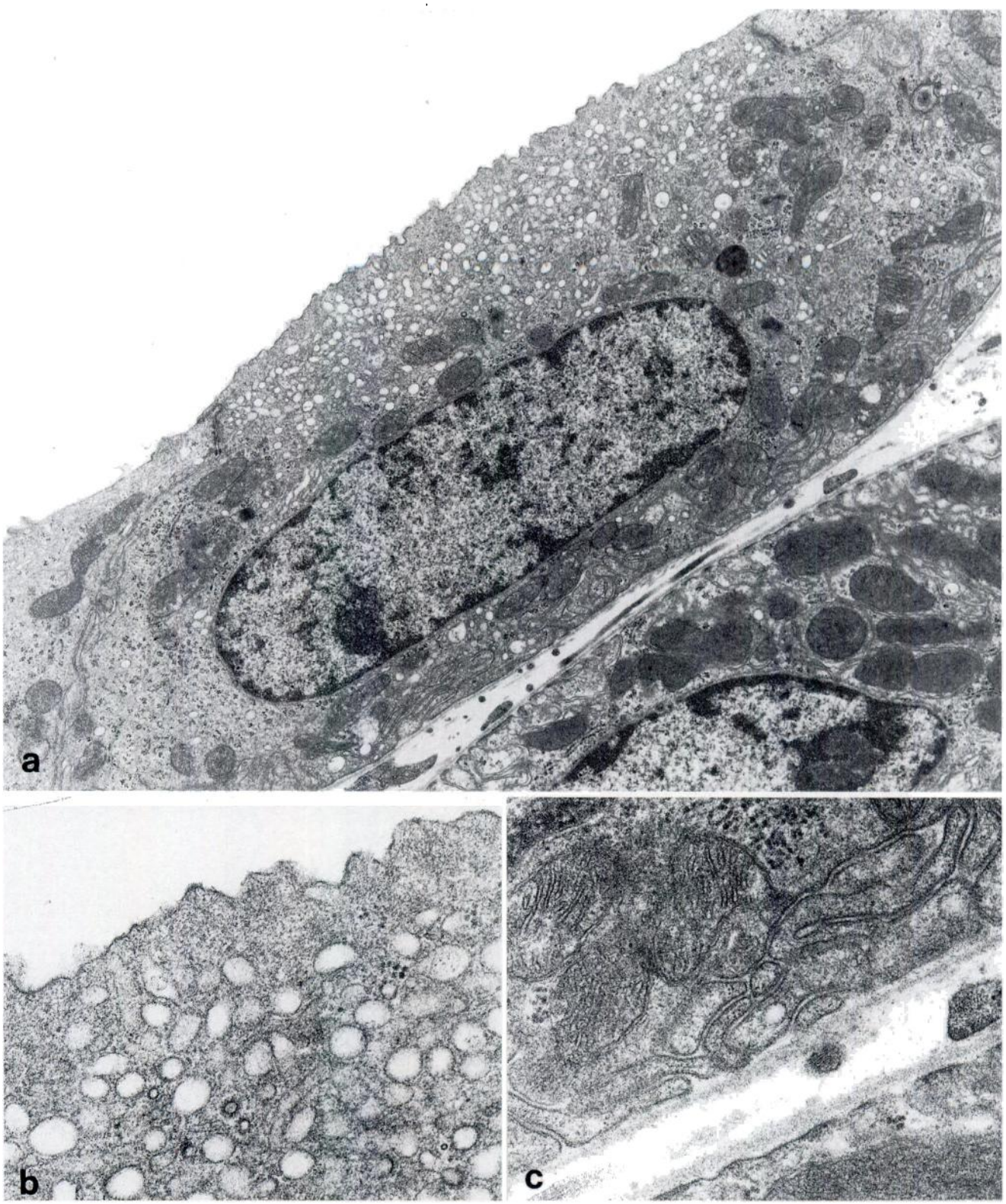

Figure 4. Transmission electron micrographs of Type B intercalated cell from the mouse CCD. The apical surface is fairly smooth and small vesicles without studs are scattered throughout the cytoplasm and are especially prevalent in the apical region of the cell (a). A gray zone free of organelles is located beneath the apical plasma membrane (b). Small studs are present on the basal plasma membrane (c). Magnification: (a) × 11,300; (b) and (c) × 42,400.

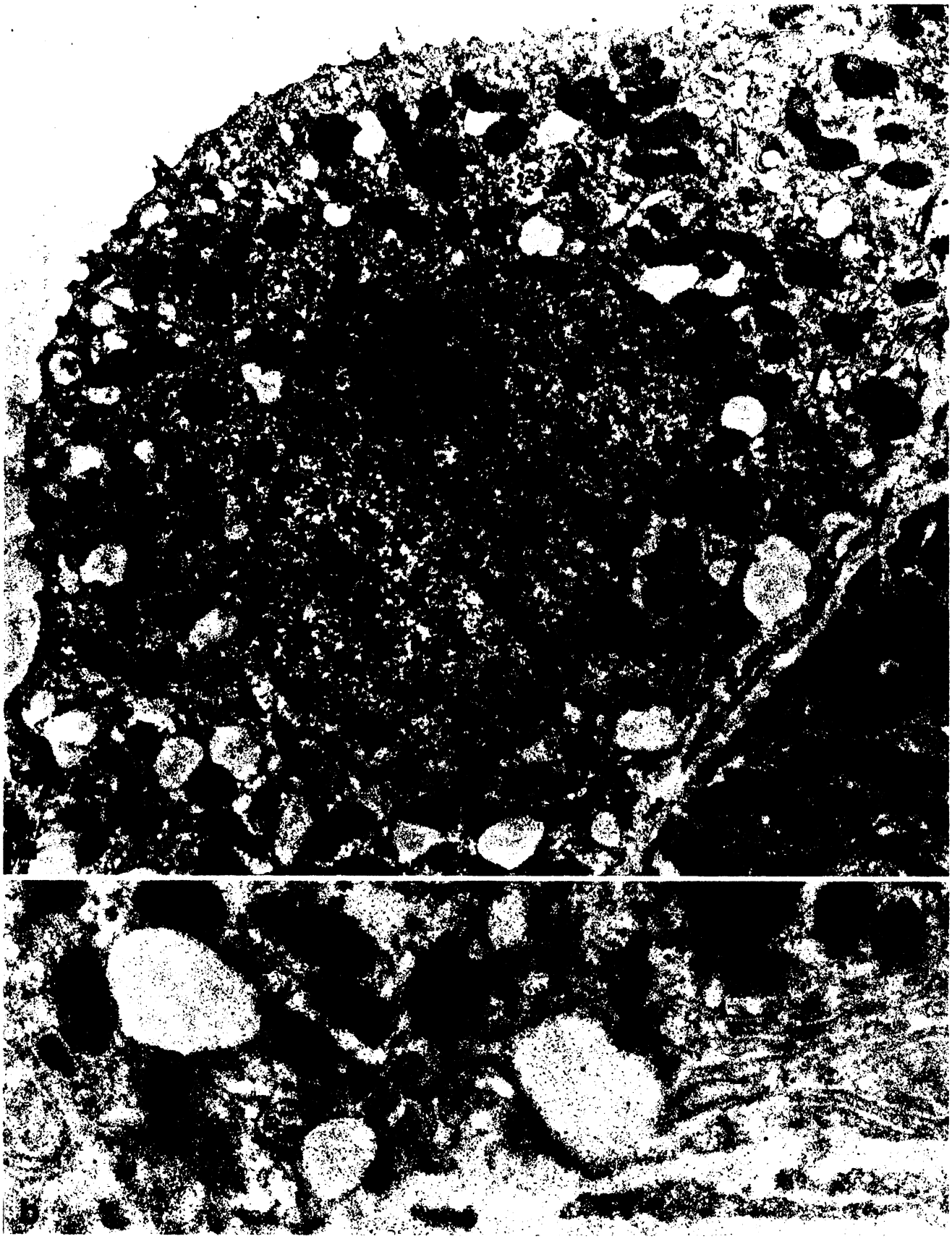

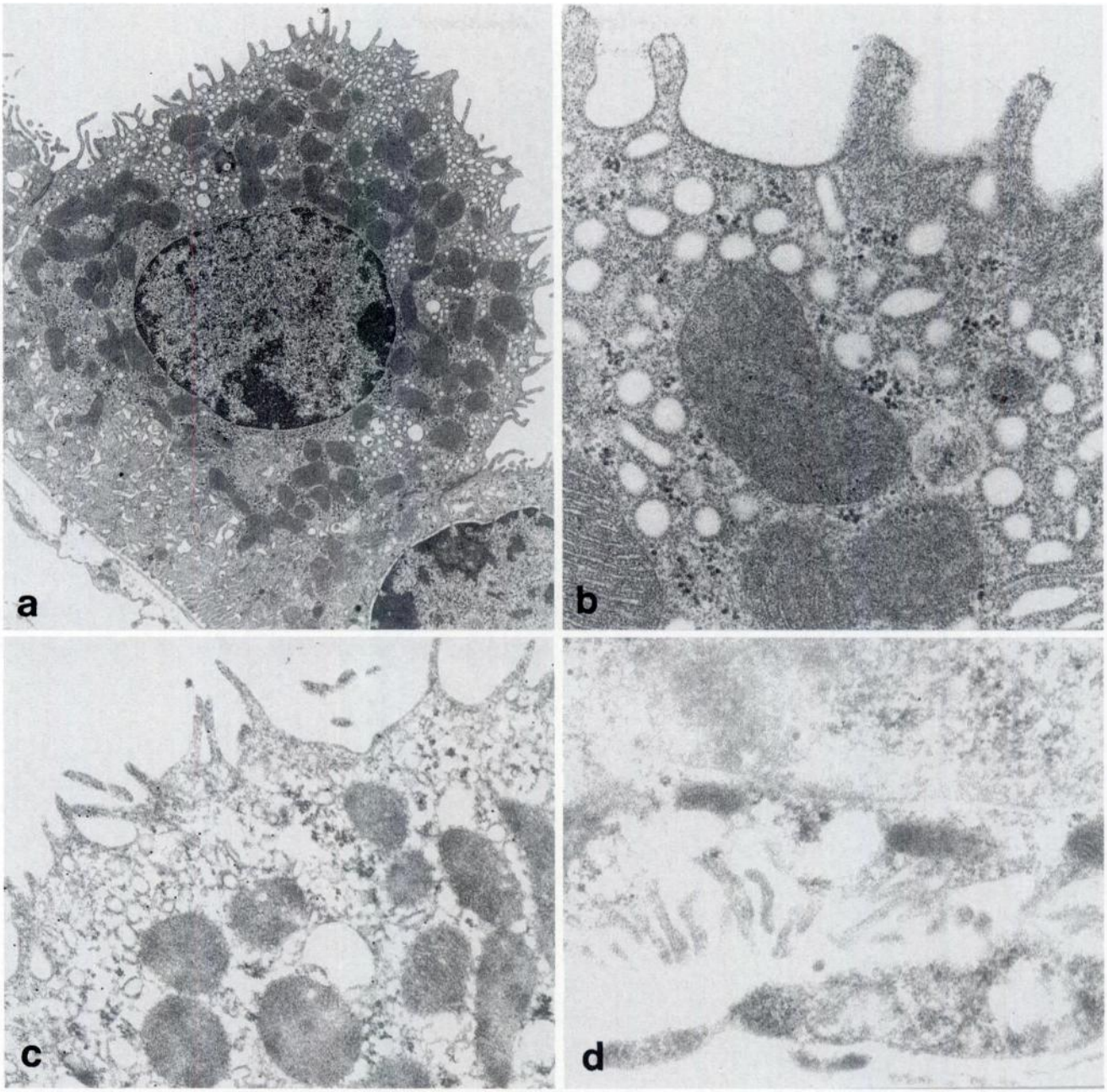

Figure 6. Transmission electron micrographs illustrating the ultrastructure (a and b) and immunogold labeling for H^+-ATPase (c) and Band 3 protein (d) of NonA-NonB type of intercalated cells in the mouse CNT. The apical plasma membrane has prominent microprojections, and numerous mitochondria and small vesicles are present throughout the cell (a). A higher magnification reveals the presence of studs on both vesicles and the apical plasma membrane (b). Immunogold labeling for H^+-ATPase is present in the apical plasma membrane and in cytoplasmic vesicles (c). There is no Band 3 immunolabel in the basolateral plasma membrane (d). Magnification: (a) × 5,200; (b) × 39,300; (c) × 21,700; (d) × 25,000.

Figure 5. Transmission electron micrographs illustrating immunogold labeling for H^+-ATPase in Type B intercalated cell in the mouse initial collecting tubule. Label for H^+-ATPase is present in cytoplasmic vesicles throughout the cell (a) and in the basolateral plasma membrane (b). Magnification: (a) × 14,300; (b) × 36,900.

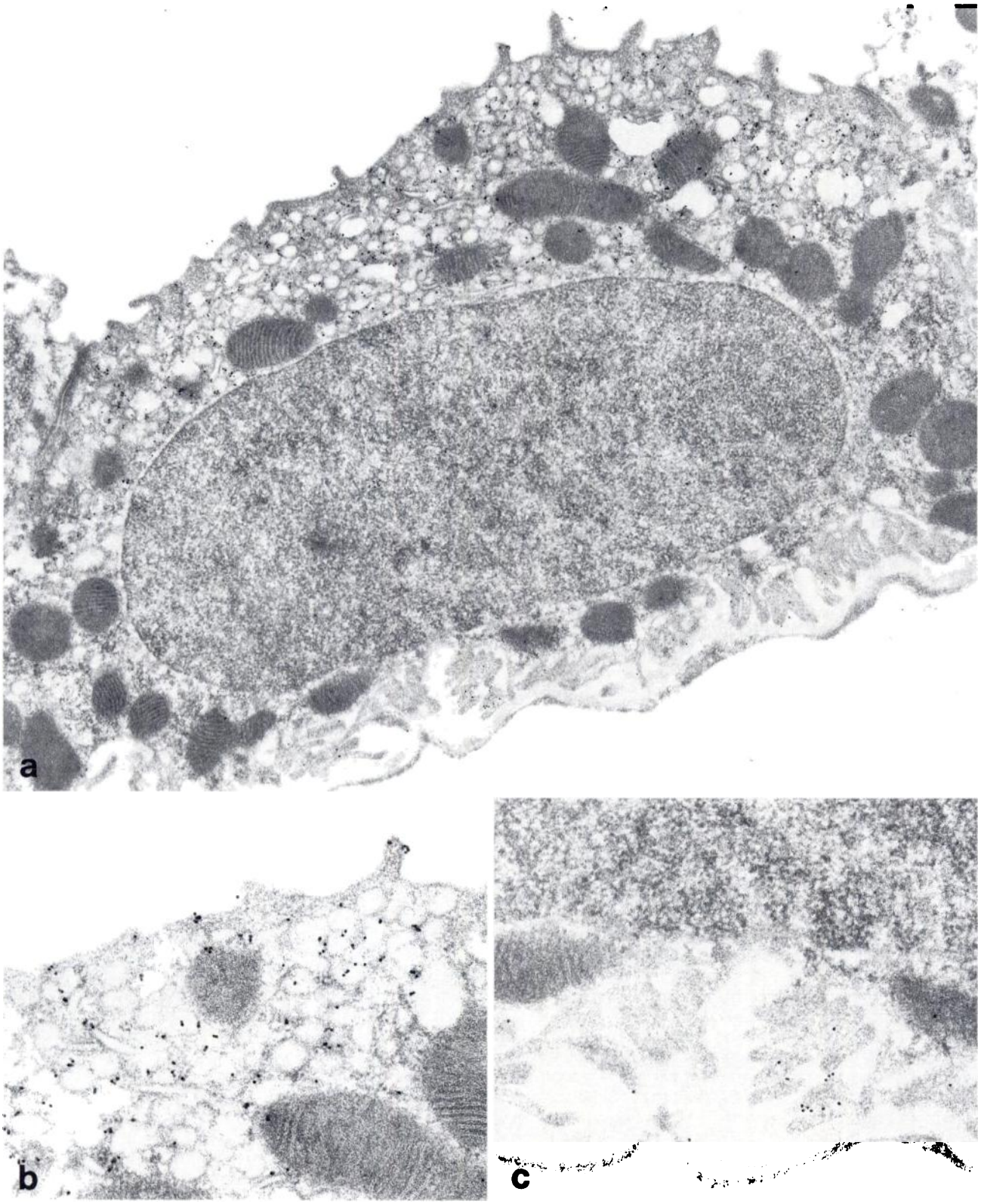
a
b
c

and the early CCD. The cells in the CNT and initial collecting tubule were larger and had a lighter cytoplasm than those in the CCD, but the ultrastructure of the cells was similar. Compared with the Type A cell, the second type of intercalated cell had a less bulging apical surface with short microprojections (Figure 4a). A distinct characteristic of this subtype was a cytoplasmic gray zone beneath the apical membrane, similar to the dense band described in Type B intercalated cells in the rat (6). This area contained filamentous components and was gray and homogeneous in appearance because of the complete absence of vesicles (Figure 4b). Tubulovesicles characteristic of Type A cells were not observed in the second cell type; however, small vesicles were dispersed throughout the remainder of the cytoplasm and were especially concentrated below the apical gray zone. These vesicles did not contain studs, and there were no studs on the apical plasma membrane. In contrast, small studs were occasionally observed on the basolateral plasma membrane (Figure 4c). Immunogold cytochemistry demonstrated labeling for H^+-ATPase on the basolateral plasma membrane and on the cytoplasmic vesicles located throughout the cell (Figures 5a and 5b). Weak labeling was also observed occasionally in vesicles close to the apical plasma membrane. There was no Band 3 immunolabeling in this population of intercalated cells.

Non A-Non B Type Intercalated Cells. The third type of intercalated cell was exclusively observed in the CNT and initial collecting tubule. It exhibited a protruding apical surface covered with microprojections similar to the A cell in these segments; however, this subtype had some additional distinct features. The cell was large, the bulging apical area above the nucleus contained numerous mitochondria, and small vesicles were distributed throughout the cytoplasm (Figure 6a). Few of these cytoplasmic vesicles had a tubular configuration, but the cytoplasmic surface of both the vesicles and the apical plasma membrane were coated with studs (Figure 6b).

Immunogold cytochemistry revealed strong labeling for H^+-ATPase on the apical plasma membrane, including the prominent microprojections on the surface, and on small cytoplasmic vesicles located primarily in the protruding apical cytoplasm (Figure 6c). There was no basolateral labeling for H^+-ATPase and no Band 3 immunoreactivity in these cells (Figure 6d).

Colocalization of H^+-ATPase and Band 3 Immunoreactivity. Experiments with a double-labeling procedure with silver enhancement of the first antibody-gold conjugate confirmed the observations made by the classic single-labeling procedure. However, with the double-labeling procedure, increased background was observed with antibodies to both H^+-ATPase and Band 3 protein. Apical labeling for H^+-ATPase and basolateral plasma membrane labeling for Band 3 protein were observed in cells with the morphologic characteristics of type A cells (Figure 7). Basolateral plasma membrane and diffuse cytoplasmic labeling for H^+-ATPase and no specific labeling for Band 3 protein were found in cells with the appearance of Type B cells. Finally, apical labeling for H^+-ATPase, but no Band 3 immunolabeling, was observed in a third population of intercalated cells located mainly in the CNT (Figure 8).

DISCUSSION

This study identified three ultrastructurally and immunologically distinct populations of intercalated cells in the mouse: Type A, Type B, and a third NonA-NonB type of intercalated cell. In both strains of mice, the intercalated cells identified by immunostaining for CA II and H^+-ATPase constituted approximately 40% of all cells in the CNT, CCD, and OMCD. This value is similar to the percentage of intercalated cells reported in both the rat and rabbit (1,2,17).

The three configurations of intercalated cells demonstrated in the mouse kidney were immunologically similar to Type A, Type B, and a third NonA-NonB type of intercalated cell described previously in the rat (10,12,22). However, the axial distribution of these cells was somewhat different from that described in the rat (10,22). Cells with apical H^+-ATPase and basolateral Band 3 protein characteristic of the Type A intercalated cell were the most frequently observed intercalated cell in the CCD, and the only type of intercalated cell present in the medullary collecting duct. Those observations are similar to results reported previously in the rat. The labeling for H^+-ATPase was located on both the apical plasma membrane and on the membrane of apical cytoplasmic vesicles as in the rat (10,13) and rabbit (16). However, Band 3 immunoreactivity was confined to the basolateral plasma membrane as in the rat (19), and was not observed in cytoplasmic vesicles or in multivesicular bodies, as it is in the rabbit (20,21).

The Type A intercalated cells in the mouse were also similar in ultrastructure to the A cells in both the rat (1,2,10) and rabbit (4,16). They contained a prominent tubulovesicular compartment beneath the apical membrane, and numerous luminal microprojections. The cytoplasmic surface of the tubulovesicles and the apical plasma membrane were coated with club-like structures or studs similar to those described previ-

Figure 7. Transmission electron micrographs illustrating immunogold colocalization of H^+-ATPase and Band 3 protein in Type A intercalated cell in mouse CCD using a silver enhancement technique. Large gold particles identifying H^+-ATPase immunolabeling are located over the apical plasma membrane and apical tubulovesicles (a and b). Small gold particles identifying Band 3 immunolabeling are located on the basolateral plasma membrane (a and c). Magnification: (a) × 20,300; (b) × 44,000; (c) × 44,000.

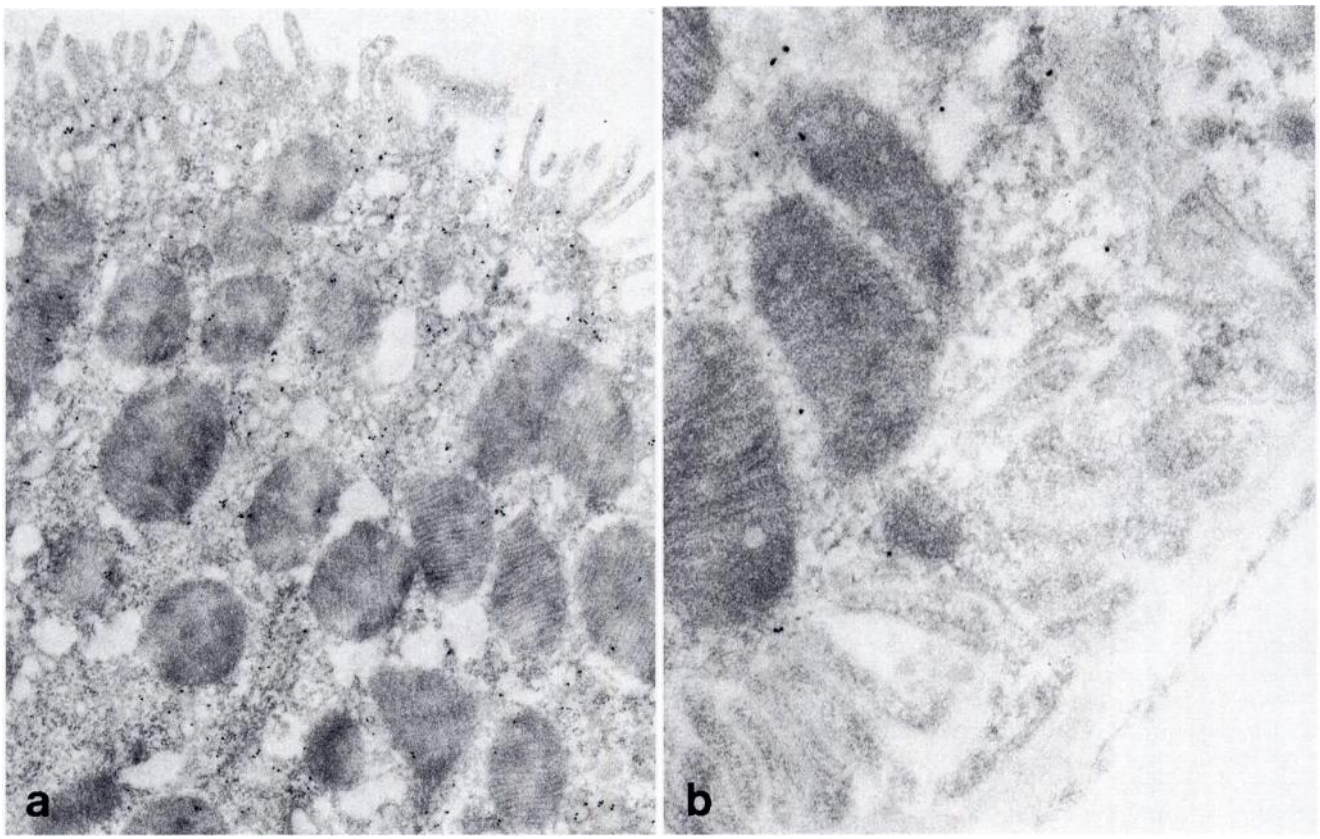

Figure 8. Transmission electron micrographs illustrating the apical (a) and basal (b) region of the same NonA-NonB type of intercalated cell from the mouse CNT after immunogold colocalization of H^+-ATPase and Band 3 protein using a silver enhancement technique. Large gold particles identifying H^+-ATPase immunolabeling are located over the apical plasma membrane and cytoplasmic vesicles (a). There is no labeling for Band 3 protein (small gold particles) over the basolateral plasma membrane (b). Magnification: (a) × 19,600; (b) × 45,500.

ously in the rat and rabbit (1–4). Immunocytochemistry studies in the rat have demonstrated that these studs contain a vacuolar-type H^+-ATPase (13). The ultrastructure of the Type A intercalated cells in the mouse varied widely from one region to another and different configurations were found even in the same tubule segment. Some cells had a rectangular shape whereas others were round because of the presence of a bulging apical surface. In the same animal, some Type A cells had few microprojections on the apical surface whereas others had numerous elongated microprojections. These differences in cell configuration most likely reflect different functional states of these cells. The observation that apical tubulovesicles are more prominent in the Type A intercalated cells in the CCD than in the intercalated cells in the medulla suggests that the cells in the cortex are in a resting state in which tubulovesicles have been internalized from the apical plasma membrane. A similar difference in the prevalence of apical tubulovesicles between intercalated cells in the CCD and OMCD exists in both the rat and rabbit (K.M. Madsen, unpublished observations).

Cells with basolateral and diffuse cytoplasmic H^+-ATPase and without Band 3 immunoreactivity characteristic of Type B intercalated cells were most frequently observed in the initial collecting tubule, but were present also in the CCD and CNT. In the CCD of the mouse, Type B cells were less common than in the CCD of the rat (2,10,12,14) and rabbit (16,17). Morphologically, they could be distinguished by the dense cytoplasmic gray zone located beneath the apical surface and by the absence of studs on the cytoplasmic surface of the vesicles. The darker-staining cytoplasm and numerous mitochondria that characterize the Type B intercalated cell in the rat and rabbit (4,6,10) were not observed in these cells in the mouse. Furthermore, the arrangement of the cytoplasmic vesicles in the B cells of the mouse was somewhat different from that described previously in the rat. Rather than being distributed diffusely throughout the cytoplasm, small vesicles without studs appeared often to be concentrated preferentially beneath the apical gray zone of the mouse Type B cell. A fine coat of studs was occasionally detected on the basolateral plasma membrane of these cells, which is in agreement with the results of the immunocytochemical study demon-

strating H^+-ATPase labeling on the basolateral membrane.

All Type B cells exhibited H^+-ATPase immunoreactivity both in the basolateral plasma membrane and in intracellular vesicles, many of which were located in the apical cytoplasm. The function of the intracellular vesicles in the B cells is not known with certainty. There is evidence that intracellular tubulovesicles might be involved in the shuttling of the H^+-ATPase between the cytoplasm and the apical plasma membrane of the Type A intercalated cells (1,2,22). However, there is little experimental evidence to support a role for vesicles in the Type B intercalated cells in the shuttling of H^+-ATPase to either the basolateral or the apical plasma membrane. Another possible role of the H^+-ATPase-positive vesicles in the B cells is an involvement in the trafficking of other transporters and possibly in their insertion into the plasma membrane.

The third type of intercalated cell, which exhibited distinct apical labeling for H^+-ATPase but no Band 3 immunoreactivity, was found only in the CNT and the initial collecting tubule. It resembled the third type of intercalated cell previously described in the rat (11,12) where it was reported to constitute less than 1% of the intercalated cells in the cortex (12). In the mouse, this configuration of intercalated cell was much more common and it had fewer mitochondria and more cytoplasmic vesicles than in the rat. The function of the NonA-NonB type of intercalated cell is not known. It is generally accepted that intercalated cells are involved in acid-base transport in the collecting duct. The Type A cells secrete protons and reabsorb bicarbonate, whereas the Type B cells secrete bicarbonate. The presence of an apical H^+-ATPase in the NonA-NonB type of intercalated cell suggests that it may be involved in proton secretion. However, it is not known if the third cell type constitutes a distinct cell population or a modified Type A cell. A subtype of intercalated cells with these particular ultrastructural features has not been described in the rabbit.

To ascertain that the NonA-NonB configuration of intercalated cell did not represent a B cell with an unusual morphology or an A cell in a tissue section with poor Band 3 antigen preservation, we performed double-immunogold labeling with silver enhancement using antibodies to both H^+-ATPase and Band 3 protein, a procedure that should identify all three populations of intercalated cells on the same section. It has been shown that the silver enhancement technique results in the gold particles being encapsulated in growing shells of silver, resulting in an increase in the size of the gold marker (29) and also effectively blocking binding to the secondary antibody (30). Therefore, immunolabeling with two different antibodies can be distinguished by the difference in the size of the gold particles. By using this technique, we verified the presence of the third cell type with apical H^+-ATPase and no Band 3 immunoreactivity in CNT segments that also contained classic Type A and Type B intercalated cells.

In the OMCD and the $IMCD_1$, all intercalated cells had the Type A configuration identified by basolateral Band 3 immunoreactivity. In contrast, in the CCD and CNT, only 60% to 65% and 35% to 40%, respectively, of the intercalated cells exhibited Band 3 immunostaining. The quantitation of intercalated cells labeled with antibodies to CA II, H^+-ATPase, and Band 3 protein did not permit us to distinguish between Type B cells and the NonA-NonB type of intercalated cells, both of which were positive for CA II and H^+-ATPase, but Band 3-negative. However, the results of the immunogold cytochemistry revealed that the NonA-NonB configuration was present mainly in the CNT, whereas the majority of the type B cells were located in the initial collecting tubule. Because the NonA-NonB configuration of the intercalated cell was not present in the CCD, it can be assumed that the Band 3-negative intercalated cells in the CCD, which constituted approximately 35% to 40% of the intercalated cells, represent Type B cells. In contrast, the Band 3-negative intercalated cells in the CNT, which constituted about 60% of the intercalated cells, included a mixture of Type B cells and NonA-NonB cells.

Recently, transgenic techniques have been used in mice to create new animal models of renal diseases as well as new renal cell lines. In transgenic mice, renal genes have been deleted or new genes have been introduced either by injection into fertilized mouse eggs or by insertion into mouse embryonic stem cells. By using these new techniques, experimental models of various renal diseases have been developed that exhibit structural as well as functional abnormalities such as glomerulosclerosis, nephron atrophy, and renal cyst formation (31–35). Moreover, renal cell lines, including a CCD (36) and an IMCD (37) cell line, have been developed from a mouse transgenic for the early region of simian virus 40. To be able to accurately evaluate the various structural abnormalities induced in these animal models and determine the phenotype of the new cell lines, it is important to be familiar with the ultrastructural and immunological characteristics of the normal mouse kidney. The results of the study presented here will serve this function with respect to the different populations of intercalated cells. Our observation provides the first evidence for the presence of three distinct subpopulations of intercalated cells in the mouse kidney and constitutes a basis for further studies of acid-base physiology in the mouse.

ACKNOWLEDGMENTS

The authors acknowledge the technical assistance of James K. Cannon, Frederick Kopp, Wendy L. Wilber, and Li Zhang. This work was supported in part by National Institutes of Health Grant AM-28330. Dr. Teng-umnuay was supported by a fellowship award from the International Society of Nephrology.

REFERENCES

1. **Madsen KM, Tisher CC:** Structural-functional relationships along the distal nephron. Am J Physiol 1986; 250(Renal Fluid Electrolyte Physiol 19):F1–F15.

2. **Tisher CC, Madsen KM:** Anatomy of the kidney. In: Brenner BM, Rector FC, Jr., Eds. The Kidney. Philadelphia: Saunders; 1990:3–75.
3. **Verlander JW, Madsen KM, Tisher CC:** Structural and functional features of proton and bicarbonate transport in the rat collecting duct. Semin Nephrol 1991;11:465–477.
4. **Kaissling B, Kriz W:** Structural analysis of the rabbit kidney. Adv Anat Embryol Cell Biol 1979;56:1–123.
5. **Crayen ML, Thoenes W:** Architecture and cell structures in the distal nephron of the rat kidney. Cytobiologie 1978;17:197–211.
6. **Madsen KM, Brenner BM:** Structure and function of the renal tubule and the interstitium. In: Tisher CC, Brenner BM, Eds. Renal Pathology with Clinical and Functional Correlations. Vol I. 2nd Ed. Lippincott: Philadelphia, 1994:661–698.
7. **Evan AP, Satlin LM, Gattone VH II, Connors B, Schwartz GJ:** Postnatal maturation of rabbit renal collecting duct. II. Morphological observations. Am J Physiol 1991; 261(Renal Fluid Electrolyte Physiol 30):F91–F107.
8. **Clapp WL, Madsen KM, Verlander JW, Tisher CC:** Intercalated cells of the rat inner medullary collecting duct. Kidney Int 1987;31:1080–1087.
9. **Kriz W, Kaissling B:** Structural organization of the mammalian kidney. In: Seldin D, Giebisch G, Eds. The Kidney: Physiology and Pathophysiology. New York: Raven Press; 1992:707–777.
10. **Verlander JW, Madsen KM, Tisher CC:** Effect of acute respiratory acidosis on two populations of intercalated cells in rat cortical collecting duct. Am J Physiol 1987; 253(Renal Fluid Electrolyte Physiol 22):F1142–F1156.
11. **Kim J, Tisher CC, Linser PJ, Madsen KM:** Ultrastructural localization of carbonic anhydrase II in subpopulations of intercalated cells of the rat kidney. J Am Soc Nephrol 1990;1:245–256.
12. **Alper SL, Natale J, Gluck S, Lodish HF, Brown D:** Subtypes of intercalated cells in rat kidney collecting duct defined by antibodies against erythroid band 3 and renal vacuolar H+ATPase. Proc Natl Acad Sci USA 1989; 86:5429–5433.
13. **Brown D, Hirsch S, Gluck S:** Localization of a proton-pumping ATPase in rat kidney. J Clin Invest 1988;82: 2114–2126.
14. **Brown D, Hirsch S, Gluck S:** An H+-ATPase in opposite plasma membrane domains in kidney epithelial cell subpopulations. Nature (Lond)1988;331:622–624.
15. **Bastani B, Purcell H, Hemken P, Trigg D, Gluck S:** Expression and distribution of renal vacuolar proton-translocating adenosine triphosphatase in response to chronic acid and alkali loads in the rat. J Clin Invest 1991;88:126–136.
16. **Verlander JW, Madsen KM, Stone DK, Tisher CC:** Ultrastructural localization of H+ATPase in rabbit cortical collecting duct. J Am Soc Nephrol 1994;4:1546–1557.
17. **Schuster VL, Fejes-Toth C, Naray-Fejes-Toth A, Gluck SL:** Colocalization of H+ATPase and band 3 anion exchanger in rabbit collecting duct intercalated cells. Am J Physiol 1991;260(Renal Fluid Electrolyte Physiol 29): F506–F517.
18. **Schuster VL, Bonsib SM, Jennings ML:** Two types of collecting duct mitochondria-rich (intercalated) cells: Lectin and band 3 cytochemistry. Am J Physiol 1986; 251(Cell Physiol 20):C347–C355.
19. **Verlander JW, Madsen KM, Low PS, Allen DP, Tisher CC:** Immunocytochemical localization of band 3 protein in the rat collecting duct. Am J Physiol 1988;255(Renal Fluid Electrolyte Physiol 24):F115–F125.
20. **Madsen KM, Kim J, Tisher CC:** Intracellular band 3 immunostaining in type A intercalated cells of rabbit kidney. Am J Physiol 1992;262(Renal Fluid Electrolyte Physiol 31):F1015–F1022.
21. **Verlander JW, Madsen KM, Cannon JK, Tisher CC:** Activation of acid-secreting intercalated cells in rabbit collecting duct with ammonium chloride loading. Am J Physiol 1994;266(Renal Fluid Electrolyte Physiol 35): F633–F645.
22. **Madsen KM, Verlander JW, Kim J, Tisher CC:** Morphological adaptation of the collecting duct to acid-base disturbances. Kidney Int 1991;40[Suppl 33]:S57–S63.
23. **Rhodin J:** Electron microscopy of the kidney. Am J Med 1958;24:661–675.
24. **Rhodin J:** Anatomy of kidney tubules. Int Rev Cytology 1958;7:485–534.
25. **Clark SL:** Cellular differentiation in the kidneys of newborn mice studied with the electron microscope. J Biophys Biochem Cytol 1957;3:349–373.
26. **Linser PJ, Sorrentino M, Moscana AA:** Cellular compartmentalization of carbonic anhydrase-C and glutamine synthetase in developing and mature mouse neural retina. Dev Brain Res 1984;13:65–71.
27. **Kim J, Welch WJ, Cannon JK, Tisher CC:** Immunocytochemical response of type A and type B intercalated cells to increased sodium chloride delivery. Am J Physiol 1992;262(Renal Fluid Electrolyte Physiol 31):F288–F302.
28. **Verlander JW, Madsen KM, Galla JH, Luke RG, Tisher CC:** Response of intercalated cells to chloride depletion metabolic alkalosis. Am J Physiol 1992;262(Renal Fluid Electrolyte Physiol 31):F309–F319.
29. **Bienz K, Egger D, Pasa Montes L:** Electron microscopic immunocytochemistry. Silver enhancement of colloidal gold marker allow double labeling with the same primary antibody. J Histochem Cytochem 1986;34:1337–1342.
30. **Holgate CS, Jackson P, Cowen PN, Bird CC:** Immunogold silver staining: New method of immunostaining with enhanced sensitivity. J Histochem Cytochem 1983;31: 938–944.
31. **Weiher H, Noda T, Gray DA, Sharpe AH, Jaenisch R:** Transgenic mouse model of kidney disease: Insertional inactivation of ubiquitously expressed gene leads to nephrotic syndrome. Cell 1990;62:425–434.
32. **Kelley KA, Agarwal N, Reeders S, Herrup K:** Renal cyst formation and multifocal neoplasia in transgenic mice carrying the simian virus 40 early region. J Am Soc Nephrol 1991;2:84–97.
33. **Lowden DA, Lindemann GW, Merlino G, Barash BD, Calvet JP, Gattone VH II:** Renal cysts in transgenic mice expressing transforming growth factor-alpha. J Lab Clin Med 1994;124:386–394.
34. **Sorenson CM, Rogers SA, Korsmeyer SJ, Hammerman MR:** Fulminant metanephric apoptosis and abnormal kidney development in bcl-2-deficient mice. Am J Physiol 1995;268(Renal Fluid Electrolyte Physiol 37): F73–F81.
35. **MacKay K, Striker LJ, Pinkert CA, Brinster RL, Striker GE:** Glomerulosclerosis and renal cysts in mice transgenic for the early region of SV40. Kidney Int 1987;32: 827–837.
36. **Stoos BA, Naray-Fejes-Toth A, Carretero OA, Ito S, Fejes-Toth G:** Characterization of a mouse cortical collecting duct cell line. Kidney Int 1991;39:1168–1175.
37. **Rauchman MI, Nigam SK, Delpire E, Gullans SR:** An osmotically tolerant inner medullary collecting duct cell line from an SV40 transgenic mouse. Am J Physiol 1993;265(Renal Fluid Electrolyte Physiol 34):F416–F424.